Solving the Schrödinger equation of hydrogen molecule with the free complement–local Schrödinger equation method: Potential energy curves of the ground and singly excited singlet and triplet states, Σ, Π, Δ, and Φ

Hiroyuki Nakashima, and Hiroshi Nakatsuji

Citation: J. Chem. Phys. **149**, 244116 (2018); doi: 10.1063/1.5060659
View online: https://doi.org/10.1063/1.5060659
View Table of Contents: http://aip.scitation.org/toc/jcp/149/24
Published by the American Institute of Physics

Solving the Schrödinger equation of hydrogen molecule with the free complement–local Schrödinger equation method: Potential energy curves of the ground and singly excited singlet and triplet states, Σ, Π, Δ, and Φ

Hiroyuki Nakashima[a] and Hiroshi Nakatsuji[a]
Quantum Chemistry Research Institute, Kyoto Technoscience Center 16, 14 Yoshida Kawaramachi, Sakyo-ku, Kyoto 606-8305, Japan

(Received 21 September 2018; accepted 3 December 2018; published online 27 December 2018)

The free-complement (FC) theory for solving the Schrödinger equation (SE) was applied to calculate the potential energy curves of the ground and excited states of the hydrogen molecule (H_2) with the $^1\Sigma_g^+$, $^1\Sigma_u^+$, $^3\Sigma_g^+$, $^3\Sigma_u^+$, $^1\Pi_g$, $^1\Pi_u$, $^3\Pi_g$, $^3\Pi_u$, $^1\Delta_g$, $^1\Delta_u$, $^3\Delta_g$, $^3\Delta_u$, $^1\Phi_g$, $^1\Phi_u$, $^3\Phi_g$, and $^3\Phi_u$ symmetries (in total, 54 states). The initial functions of the FC theory were formulated based on the atomic states of the hydrogen atom and its positive and negative ions at the dissociation limits. The local Schrödinger equation (LSE) method, which is a simple sampling-type integral-free methodology, was employed instead of the ordinary variational method and highly accurate results were obtained stably and smoothly along the potential energy curves. Thus, with the FC-LSE method, we succeeded to perform the comprehensive studies of the H_2 molecule from the ground to excited states belonging up to higher angular momentum symmetries and from equilibriums to dissociation limits with almost satisfying spectroscopic accuracy, i.e., 10^{-6} hartree order around 1 cm^{-1}, as absolute solutions of the SE by moderately small calculations. *Published by AIP Publishing.*
https://doi.org/10.1063/1.5060659

I. INTRODUCTION

The hydrogen molecule (H_2) is the simplest molecule but has fundamental importance in molecular physics and chemistry. In 1927, Heitler and London[1] first applied quantum mechanics to this molecule. Their calculations were successful in describing chemical bonding of the H_2 molecule and became the origin of the valence bond theory. Since this pioneering work, the H_2 molecule had been a benchmark for many quantum chemistry theories.[2–21] In 1933, James and Coolidge[2,3] reported accurate calculations on the elliptic coordinates including the explicitly correlated r_{12} terms, whose importance was first shown by Hylleraas for the helium atom.[22] In 1960, Kolos and Roothaan[4,5] computed the accurate potential energy curves for the ground and a few low-lying excited states with the extended James-Coolidge method. In 1961, Davidson[4] also computed these states and obtained the improved results. Since 1964, Kolos, Wolniewicz, and coworkers[5–12] performed systematic studies on the ground and low-lying excited states even with Π and Δ symmetries. Liu, Hagstrom, and Sims[13–15] employed the modified Kolos and Wolniewicz wave functions and provided accurate wave functions of the ground state and several excited states. Rychlewski, Cencek, Komasa *et al.*[16–18] employed the explicitly correlated Gaussian or Slater functions and reported further accurate solutions for the ground state. Clementi and Corongiu[19] reported the potential energy curves of the ground and 14 excited states belonging to the $^1\Sigma_g^+$ state up to very long inter-nuclear distances near the dissociation limits. They employed ordinary Slater- and Gauss-type orbital expansion methods. However, due to the absence of the r_{12} terms, the absolute energies were less accurate than those using r_{12} terms explicitly. Recently, Pachucki[20,21] developed integration schemes for the James-Coolidge functions and reported as benchmark calculations the current best variational energies for the limited number of inter-nuclear distances belonging to the $^1\Sigma_g^+$ symmetry.

On another front, we have proposed the free-complement (FC) theory for exactly solving the Schrödinger equation (SE)[23–30] with applications to several atoms and molecules.[31–37] The FC wave function ψ is written in the form[24]

$$\psi = \sum_I c_I \phi_I, \tag{1}$$

where $\{\phi_I\}$, referred to as complement functions (cf's), are generated by applying the system's Hamiltonian and g function (necessary to avoid Coulomb singularities) several times to some initial function ψ_0. This FC ψ is guaranteed to be converging to the exact solution with increasing iteration or order of the FC theory.[24] In this paper, we apply the FC theory to the calculations of the potential energy curves of ground and excited states of H_2. We studied them with two alternative ways by using the variational method or local Schrödinger equation (LSE) method[26,29] to determine the variables $\{c_I\}$ in Eq. (1). In the former case,[36,37] the matrix elements were evaluated using analytical integrations and the results were stable with satisfying Ritz-variational property. In this case, however,

[a]Electronic addresses: h.nakashima@qcri.or.jp and h.nakatsuji@qcri.or.jp

because of their easy integration scheme, the James-Coolidge type functions were employed as ψ_0 on the elliptic coordinates $\lambda_i = (r_{iA} + r_{iB})/R$, $\mu_i = (r_{iA} - r_{iB})/R$, where r_{iA} and r_{iB} denote the inter-nuclear distances between electron i and H_A and H_B atoms, respectively, and R is the inter-nuclear distance. λ_i and μ_i are two-center coordinates and cannot be directly mapped to the atomic local coordinates at dissociation. These often cause numerical instabilities at long-distant R and/or for highly excited states. Alternatively, in the present paper, we employed the LSE method,[26,29] which is a sampling-type integral-free methodology, instead of the ordinary variational method. In this case, although some information about sampling points is necessary, any functions and coordinates are available in principle appropriately to represent physical natures of the system. Therefore, we employ the local atomic coordinates r_{iA} and r_{iB} and construct ψ_0 considering the atomic states at the dissociations of target electronic states from the neutral hydrogen atom and its positive (H^+) and negative ions (H^-). The LSE method can also avoid huge computational effort for evaluating analytical integrations and can be easily parallelized.[26,29]

The present system is a good candidate to examine the potentiality of the FC theory and the utility of the LSE method as one of the simplest examples. The present purpose is not to perform a landmark calculation that pursues highly accurate digits only targeting the ground and/or a few excited states but to study the H_2 molecule comprehensively for the ground and many excited states from bonding regions to dissociation limits with satisfying spectroscopic accuracy, i.e., 10^{-6} hartree order around 1 cm^{-1}, as absolute solutions of the SE by moderately small calculations. We report totally 54 states belonging to the $^1\Sigma_g^+$, $^1\Sigma_u^+$, $^3\Sigma_g^+$, $^3\Sigma_u^+$, $^1\Pi_g$, $^1\Pi_u$, $^3\Pi_g$, $^3\Pi_u$, $^1\Delta_g$, $^1\Delta_u$, $^3\Delta_g$, $^3\Delta_u$, $^1\Phi_g$, $^1\Phi_u$, $^3\Phi_g$, and $^3\Phi_u$ symmetries and their potential energy curves.

II. FC-LSE CALCULATIONS AND COMPUTATIONAL DETAILS

A. Initial functions

Constructing appropriate initial functions in the FC theory is practically important for efficiently calculating the exact solutions. As an objective of the present paper, we describe the accurate potential energy curves for the ground and various excited states with guaranteed dissociation limits. The wave functions constructed on the local Heitler-London-Slater-Pauling (HLSP) structures should match this purpose rather than Hartree-Fock (molecular orbitals) wave functions or the two-center James-Coolidge type functions, which cannot describe correct dissociations. Since the solutions of the one-electron hydrogen atom are exactly known, the covalent dissociations are correctly guaranteed. For the ionic structures (H^-H^+), although the exact solutions of H^- are not known, accurate descriptions are possible with higher FC order. In the present study, we calculate the states corresponding to the covalent dissociations of principal quantum number n = 1, 2, 3, and 4 with s, p, d, and f symmetries and also the lowest ionic state. The employed spatial initial functions are denoted by

$$
\begin{aligned}
\Sigma: \quad \psi_0^{\Sigma} &= SA\left[\varphi_{1s}^{(H_A)}\varphi_{1s}^{(H_B)} + \varphi_{1s}^{(H_A)}\varphi_{1s}^{(H_A)} + \sum_{n=2}^{4}\varphi_{1s}^{(H_A)}\varphi_{ns}^{(H_B)} + \sum_{n=2}^{4}\varphi_{1s}^{(H_A)}\varphi_{np_z}^{(H_B)} + \sum_{n=3}^{4}\varphi_{1s}^{(H_A)}\varphi_{nd_{z^2}}^{(H_B)} + \varphi_{1s}^{(H_A)}\varphi_{4f_{z^3}}^{(H_B)}\right],\\
\Pi: \quad \psi_0^{\Pi} &= SA\left[\sum_{n=2}^{4}\varphi_{1s}^{(H_A)}\varphi_{np_x}^{(H_B)} + \sum_{n=3}^{4}\varphi_{1s}^{(H_A)}\varphi_{nd_{xz}}^{(H_B)} + \varphi_{1s}^{(H_A)}\varphi_{4f_{xz^2}}^{(H_B)}\right],\\
\Delta: \quad \psi_0^{\Delta} &= SA\left[\sum_{n=3}^{4}\varphi_{1s}^{(H_A)}\varphi_{nd_{xy}}^{(H_B)} + \varphi_{1s}^{(H_A)}\varphi_{4f_{xyz}}^{(H_B)}\right],\\
\Phi: \quad \psi_0^{\Phi} &= SA\left[\varphi_{1s}^{(H_A)}\varphi_{4f_{x^2y}}^{(H_B)}\right]
\end{aligned}
\tag{2}
$$

for Σ, Π, Δ, and Φ symmetries, respectively, and each term in the parentheses consists of (function of electron 1) × (function of electron 2). φ_q represents the exact hydrogen-atom wave functions, where q is 1s, 2s, 2p, 3s, 3p, 3d, 4s, 4p, 4d, and 4f orbitals and the molecular axis is set to the z axis. S is the spatial-symmetry operator and A is the spin-symmetry (singlet or triplet) and antisymmety operator. These are listed as follows:

$$
\begin{aligned}
&^1\Sigma_g^+, {}^1\Pi_u, {}^1\Delta_g, {}^1\Phi_u: \quad S = 1 + P_{AB}, \quad A = 1 + P_{12},\\
&^1\Sigma_u^+, {}^1\Pi_g, {}^1\Delta_u, {}^1\Phi_g: \quad S = 1 - P_{AB}, \quad A = 1 + P_{12},\\
&^3\Sigma_g^+, {}^3\Pi_u, {}^3\Delta_g, {}^3\Phi_u: \quad S = 1 - P_{AB}, \quad A = 1 - P_{12},\\
&^3\Sigma_u^+, {}^3\Pi_g, {}^3\Delta_u, {}^3\Phi_g: \quad S = 1 + P_{AB}, \quad A = 1 - P_{12}.
\end{aligned}
\tag{3}
$$

For $^1\Sigma_g^+$ symmetry, $\varphi_{1s}^{(H_A)}(1)\varphi_{1s}^{(H_B)}(2)$ represents the most important covalent form for the ground state of H_2, where electron 1 belongs to the 1s orbital of hydrogen atom H_A

and electron 2 also belongs to the 1s orbital of hydrogen atom H_B. $\varphi_{1s}^{(H_A)}\varphi_{2s}^{(H_B)}$ to $\varphi_{1s}^{(H_A)}\varphi_{4s}^{(H_B)}$ terms are introduced for the correct dissociations to the atomic 2s, 3s, and 4s Rydberg excited states, where electron 2 occupies 2s to 4s orbitals on the H_B atom. Although p, d, and f orbitals are orthogonal to s orbitals in the atomic case, some of them also mix in the same spatial symmetry in the molecular case. Therefore, $\varphi_{1s}^{(H_A)}\varphi_{2p_z}^{(H_B)}$ to $\varphi_{1s}^{(H_A)}\varphi_{4p_z}^{(H_B)}$, $\varphi_{1s}^{(H_A)}\varphi_{3d_{z^2}}^{(H_B)}$ to $\varphi_{1s}^{(H_A)}\varphi_{4d_{z^2}}^{(H_B)}$, and $\varphi_{1s}^{(H_A)}\varphi_{4f_{z^3}}^{(H_B)}$ terms were also employed for $^1\Sigma_g^+$ symmetry and they dissociate to the atomic 2p, 3p, 4p, 3d, 4d, and 4f Rydberg states. The second term of $^1\Sigma_g^+$ in Eq. (2) $\varphi_{1s}^{(H_A)}\varphi_{1s}^{(H_A)}$ represents an ionic contribution. Although the atomic energy level of H^- is rather higher than the above Rydberg dissociations, it significantly influences binding properties and shapes of the potential energy curves. We omitted the terms corresponding to double Rydberg excitation or the Rydberg ionic term, like $\varphi_{2s}^{(H_A)}\varphi_{2s}^{(H_B)}$ or $\varphi_{1s}^{(H_A)}\varphi_{2s}^{(H_A)}$, since they have very high energies out of scale of the present targets. Thus, totally 11 terms were employed as initial functions for $^1\Sigma_g^+$ symmetry.

The initial functions for $^1\Sigma_u^+$, $^3\Sigma_g^+$, and $^3\Sigma_u^+$ symmetries were similarly constructed to the $^1\Sigma_g^+$ case. However, from symmetric restrictions due to spin function and antisymmetry rule by A, the dissociation channels to the same H_A and H_B states disappear for $^1\Sigma_u^+$ and $^3\Sigma_g^+$; then, the first term $\varphi_{1s}^{(H_A)}\varphi_{1s}^{(H_B)}$ is unnecessary for these symmetries. The lowest states of $^1\Sigma_g^+$ and $^3\Sigma_u^+$, therefore, only describe the homopolar dissociations to the ground states ($1s$ states) of the hydrogen atom. Similarly, the ionic contribution of the ground-state H^- cannot be allowed for the triplet states; then, the second term $\varphi_{1s}^{(H_A)}\varphi_{1s}^{(H_A)}$ is unnecessary for $^3\Sigma_g^+$ and $^3\Sigma_u^+$. For Π, Δ, and Φ symmetries, the initial functions are also similarly constructed, but they are much simpler than the Σ symmetry case because both the ground-state dissociation channel and the ionic contribution are unnecessary and, therefore, double occupied configurations do not exist.

We report totally 54 states and their potential energy curves: 7, 6, 6, and 7 states for $^1\Sigma_g^+$, $^1\Sigma_u^+$, $^3\Sigma_g^+$, and $^3\Sigma_u^+$ (26 states for Σ symmetry), all 4 states for $^1\Pi_g$, $^1\Pi_u$, $^3\Pi_g$, and $^3\Pi_u$ (16 states for Π symmetry), all 2 states for $^1\Delta_g$, $^1\Delta_u$, $^3\Delta_g$, and $^3\Delta_u$ (8 states for Δ symmetry), and all one states for $^1\Phi_g$, $^1\Phi_u$, $^3\Phi_g$, and $^3\Phi_u$ (4 states for Φ symmetry). In these states, however, only a single state in each symmetry is included for the states of principal quantum number $n = 4$ at dissociation because some sampling ambiguities were caused in higher excited states for which initial functions of $n = 5$ states and more sampling points may be required.

B. FC-LSE calculations

We generated the cf's by applying the Hamiltonian and g function to the initial functions. The g function used here is given by

$$g = r_{1A} + r_{1B} + r_{2A} + r_{2B} + r_{12}, \tag{4}$$

where r_{iA} and r_{iB} denote the inter-nuclear distances between electron i and H_A and H_B atoms and r_{12} denotes the inter-electron distance of electrons 1 and 2. In the case electron 1 belongs to the orbital centered on the H_A atom, r_{1B} is considered as the inter-atomic coordinate and works for polarization effect and also satisfies the inter-atomic cusp condition. This term might not be important for general molecules because of the locality of the wave function but, in the case of hydrogen, it is effective due to its small inter-nuclear distance. In variational calculations, the integrations for r_{iB} terms are generally not easy, but these are treated in the LSE method without difficulty. We performed the FC-LSE calculations at the order 4 and order 6 only for $\varphi_{1s}^{(H_A)}\varphi_{1s}^{(H_B)}$ which is important for the ground-state dissociation channel. The numbers of generated cf's $\{\phi_I\}$ are 1450, 1204, 1134, and 1380 for $^1\Sigma_g^+$, $^1\Sigma_u^+$, $^3\Sigma_g^+$, and $^3\Sigma_u^+$, respectively, and 756, 378, and 126 for Π, Δ, and Φ, respectively.

The LSE method was employed to determine $\{c_I\}$ in Eq. (1). In some choices of the LSE method, we employed the HS method.[26,29] In the HS method, we solve the secular equation $\mathbf{HC} = \mathbf{SCE}$, where $\mathbf{H}_{ij} = \sum_\mu \phi_i(r_\mu) \cdot H\phi_j(r_\mu)$ and $\mathbf{S}_{ij} = \sum_\mu \phi_i(r_\mu) \cdot \phi_j(r_\mu)$ with r_μ denoting the sampling point. This has a non-symmetric form of the eigenvalue equation with symmetric $\mathbf{S}$ and non-symmetric $\mathbf{H}$. It is a method to match to the conventional variational method with increasing sampling and a single diagonalization for each symmetry provides the solutions for all states simultaneously from the lowest to higher excited states. Therefore, the state- and Hamiltonian-orthogonalities among solutions are guaranteed on the space of sampling coordinates. They are the necessary conditions of the SE and significant to describe correct relations among ground and excited states.

C. Sampling points

In the LSE method, it is also necessary to prepare appropriate sampling points adapting to quantum mechanical highly accurate calculations to reduce statistical ambiguities as much as possible. In Ref. 29, we extensively examined the nature of sampling points for the LSE method. As a conclusion, the distribution of sampling points should have similar amplitudes to the electron distributions of the target states. Since we need to calculate not only the valence but also the Rydberg-type higher excited states, widely distributed sampling points are necessary. For the present purpose, we employed a Metropolis scheme[38] starting from the local sampling points.[27,29] We first prepared the sampling distribution by the local sampling method according to the densities $\left|\varphi_{1s}^{(H_A)}\varphi_{1s}^{(H_B)}\right|^2$, $\left|\varphi_{1s}^{(H_A)}\varphi_{2s}^{(H_B)}\right|^2$, $\left|\varphi_{1s}^{(H_A)}\varphi_{3s}^{(H_B)}\right|^2$, $\left|\varphi_{1s}^{(H_A)}\varphi_{4s}^{(H_B)}\right|^2$, and $\left|\varphi_{1s}^{(H_A)}\varphi_{1s}^{(H_A)}\right|^2$ which belong to totally symmetric $^1\Sigma_g^+$, corresponding to $n = 1$–4 and ionic contribution, for each 1×10^6 sampling points. Starting with this initial sampling distribution, we constructed totally 5×10^6 sampling points using the Metropolis scheme[38] according to the density function γ given by

$$\gamma = \left|(1 + P_{AB})(1 + P_{12})\left[\varphi_{1s}^{(H_A)}\varphi_{1s}^{(H_B)} + \varphi_{1s}^{(H_A)}\varphi_{2s}^{(H_B)} + \varphi_{1s}^{(H_A)}\varphi_{3s}^{(H_B)} + \varphi_{1s}^{(H_A)}\varphi_{4s}^{(H_B)} + \varphi_{1s}^{(H_A)}\varphi_{1s}^{(H_A)}\right]\right|^2, \tag{5}$$

where this γ includes spatial and spin symmetric and electron antisymmetry effects. At each R for the potential energy curves, we independently generated the sampling points using the above local sampling and Metropolis scheme. The continuity about sampling points at each R, therefore, is not

strictly satisfied. Nevertheless, the present results, discussed in Sec. III, were sufficiently accurate and showed smooth potential energy curves, where statistical fluctuations appeared in negligible digits of absolute energies.

III. POTENTIAL ENERGY CURVES OF THE GROUND AND LOW-LYING EXCITED STATES

Figure 1 shows the potential energy curves of the ground state $1^1\Sigma_g^+$ and the lowest state of $^3\Sigma_u^+$. Only these states covalently dissociate to the 1s orbitals of the hydrogen atom, H(1s) + H(1s). Figures 2–17 represent the potential energy curves of the $^1\Sigma_g^+$, $^1\Sigma_u^+$, $^3\Sigma_g^+$, $^3\Sigma_u^+$, $^1\Pi_g$, $^1\Pi_u$, $^3\Pi_g$, $^3\Pi_u$, $^1\Delta_g$, $^1\Delta_u$, $^3\Delta_g$, $^3\Delta_u$, $^1\Phi_g$, $^1\Phi_u$, $^3\Phi_g$, and $^3\Phi_u$ symmetries, respectively, except for the lowest states $1^1\Sigma_g^+$ and $1^3\Sigma_u^+$. Figures 18 and 19 summarize all the calculated curves with the regions of R = 0.0–20.0 a.u. and R = 0.0–100.0 a.u., respectively, except for $1^1\Sigma_g^+$ and $1^3\Sigma_u^+$ since they locate the lower energy region. Figures S1 and S2 give the plots also including the $1^1\Sigma_g^+$ and $1^3\Sigma_u^+$ states. Table I summarizes the calculated absolute energies by this work compared with those by the other calculations in the literature[6,7,15,19–21] for the $^1\Sigma_g^+$ symmetry. All the calculated energies of the potential energy curves and the H-square errors defined in Ref. 29 are available in Tables S1–S16 in the supplementary material. The H-square error is a good indicator to examine the accurateness of the wave function. It is easily evaluated in the LSE method, whereas the variational method requires difficult integrations of the square root of the Hamiltonian.

As shown in Table I, Figs. 1–19, Tables S1–S16, and Figs. S1 and S2, we were successful in obtaining highly accurate potential energy curves from the ground to various excited states with the FC-LSE method. Comparing the calculated energies $E_{\text{FC-LSE}}$ with those from the references $E_{\text{Ref.}}$, their absolute energy differences $\Delta E = E_{\text{FC-LSE}} - E_{\text{Ref.}}$ from the most accurate references by Pachucki[20,21] were 10^{-6} hartree order almost less than 1 cm^{-1} satisfying spectroscopic accuracy for the states at several R whose reference values are available. When comparing to other old Refs. 6 and 7, ΔE at several R for some states were 10^{-4}-10^{-5} hartree order, but our results would be expected to be more accurate than those. In spite of long theoretical studies of H_2, there were no accurate theoretical results in the literature for some highly excited states and they were first calculated in the present study.

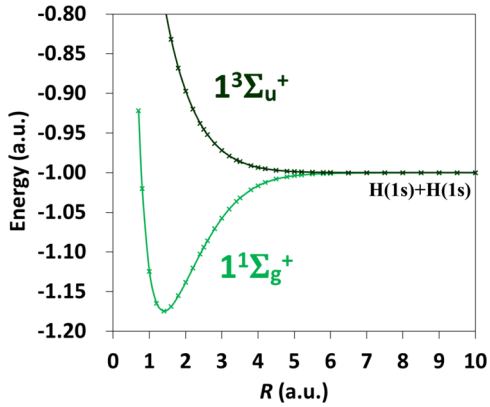

FIG. 1. Potential energy curves of the ground state $1^1\Sigma_g^+$ and the lowest state of $^3\Sigma_u^+$. Both states dissociate to the 1s orbitals of the hydrogen atom. The figure is plotted with the region of R = 0.0–10.0 a.u.

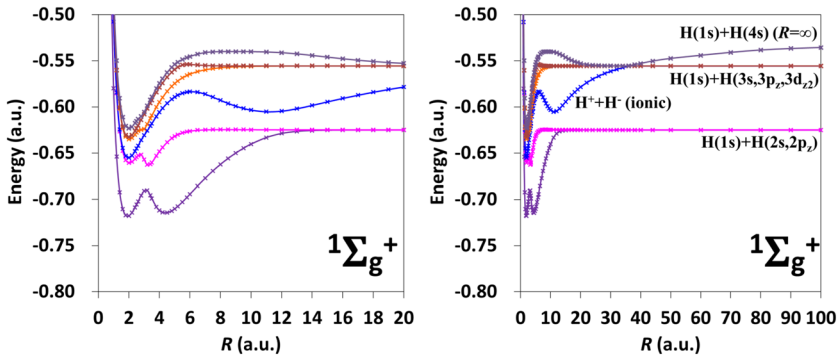

FIG. 2. Potential energy curves of the six lower excited states of $^1\Sigma_g^+$ with the energy region of −0.5 to −0.8 a.u. The ground state locates the lower energy region out of range. The left and right figures are plotted with the regions of R = 0.0–20.0 a.u. and R = 0.0–100.0 a.u., respectively.

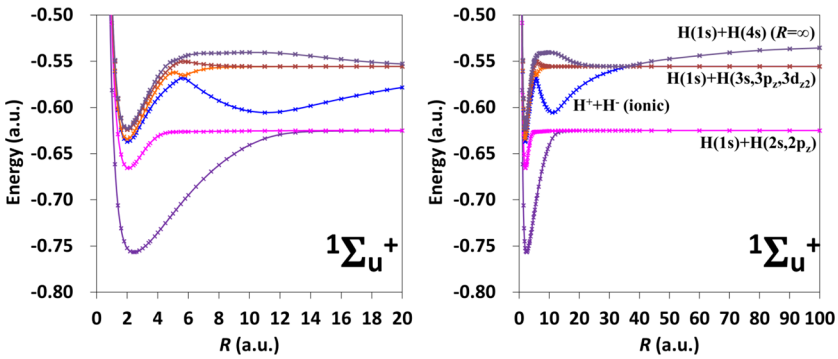

FIG. 3. Potential energy curves of the six lower excited states of $^1\Sigma_u^+$ with the energy region of −0.5 to −0.8 a.u. The left and right figures are plotted with the regions of R = 0.0–20.0 a.u. and R = 0.0–100.0 a.u., respectively.

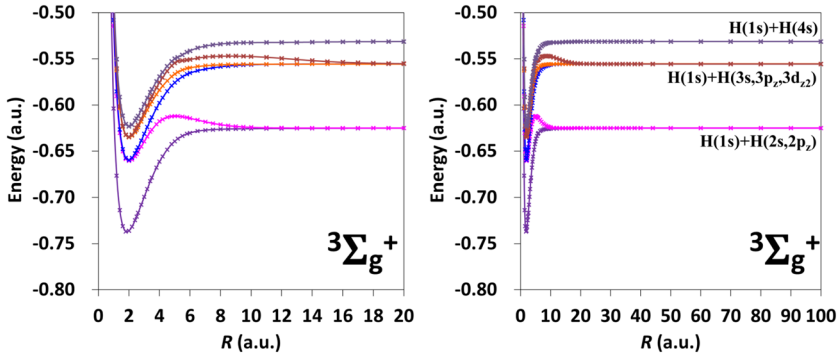

FIG. 4. Potential energy curves of the six lower excited states of $^3\Sigma_g^+$ with the energy region of −0.5 to −0.8 a.u. The left and right figures are plotted with the regions of R = 0.0–20.0 a.u. and R = 0.0–100.0 a.u., respectively.

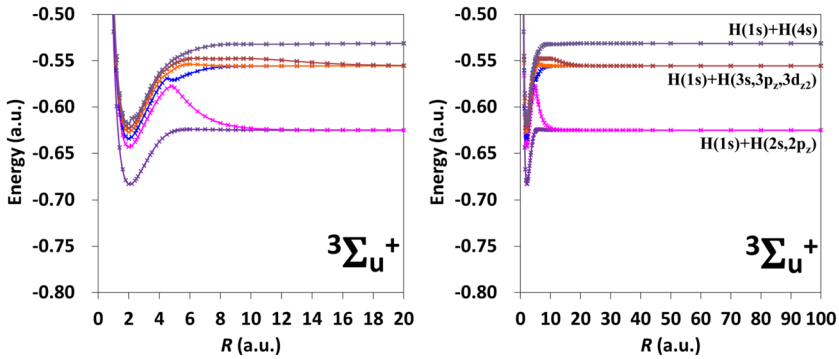

FIG. 5. Potential energy curves of the six lower excited states of $^3\Sigma_u^+$ with the energy region of −0.5 to −0.8 a.u. The lowest state dissociates to the 1s orbital of the hydrogen atom and locates the lower energy region out of range. The left and right figures are plotted with the regions of R = 0.0–20.0 a.u. and R = 0.0–100.0 a.u., respectively.

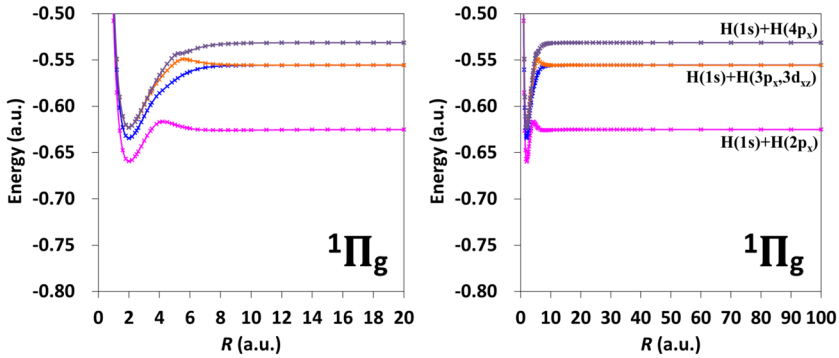

FIG. 6. Potential energy curves of the four lower excited states of $^1\Pi_g$ with the energy region of −0.5 to −0.8 a.u. The left and right figures are plotted with the regions of R = 0.0–20.0 a.u. and R = 0.0–100.0 a.u., respectively.

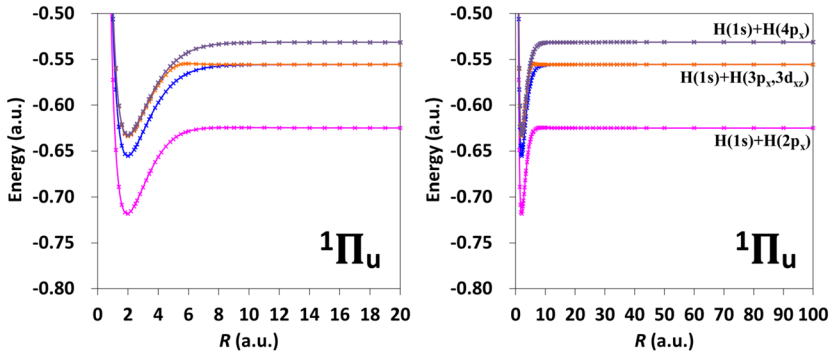

FIG. 7. Potential energy curves of the four lower excited states of $^1\Pi_u$ with the energy region of −0.5 to −0.8 a.u. The left and right figures are plotted with the regions of R = 0.0–20.0 a.u. and R = 0.0–100.0 a.u., respectively.

Thus, there was no integration difficulty in the LSE method even for higher excited states, long distant R, and the states belonging to higher angular momentum symmetries. The computation algorithm of the LSE method is simple and can be easily parallelized. For the $^1\Sigma_g^+$ symmetry which has the largest number of the complement functions, we needed about 15 min computation at each R with 1 node (28 core) using PRIMERGY CX2550 at the Research Centre for Computational Science, Okazaki, Japan. Therefore, it was almost a one-day job for all the calculations to describe the potential energy curves.

In Subsections III A–III E, we will individually discuss the potential energy curves of each state and symmetry in more detail.

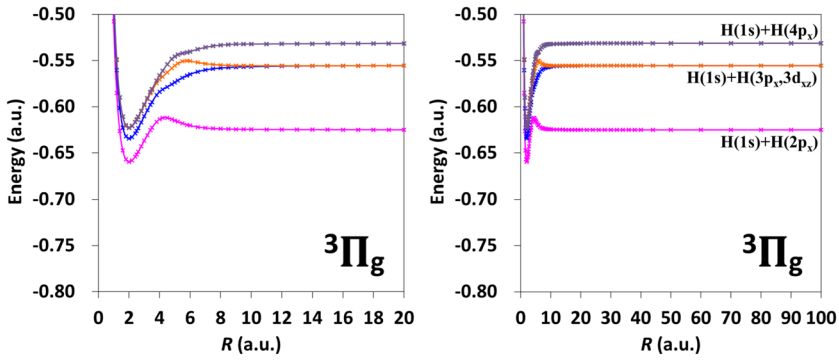

FIG. 8. Potential energy curves of the four lower excited states of $^3\Pi_g$ with the energy region of −0.5 to −0.8 a.u. The left and right figures are plotted with the regions of R = 0.0–20.0 a.u. and R = 0.0–100.0 a.u., respectively.

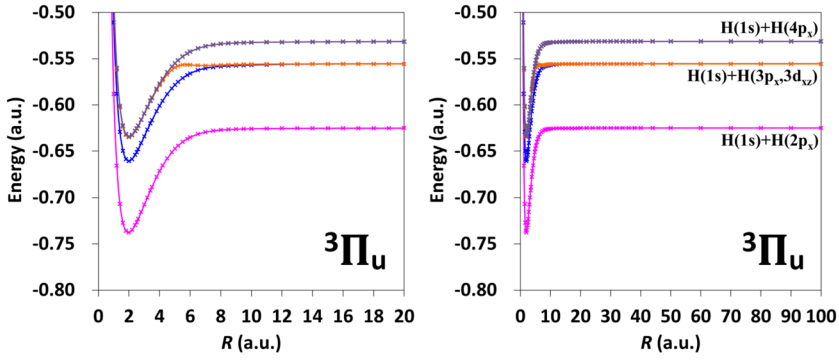

FIG. 9. Potential energy curves of the four lower excited states of $^3\Pi_u$ with the energy region of −0.5 to −0.8 a.u. The left and right figures are plotted with the regions of R = 0.0–20.0 a.u. and R = 0.0–100.0 a.u., respectively.

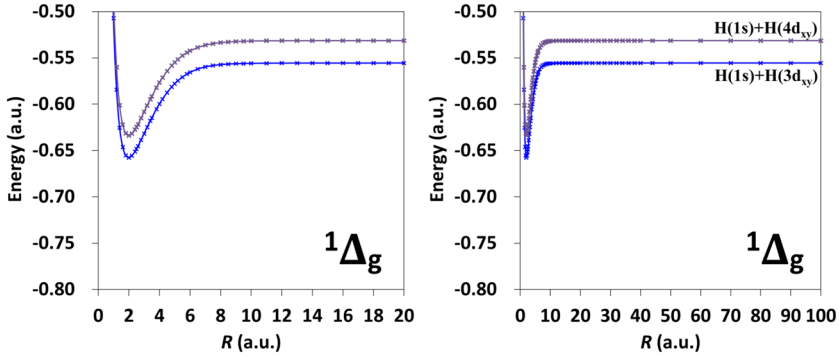

FIG. 10. Potential energy curves of the two lower excited states of $^1\Delta_g$ with the energy region of −0.5 to −0.8 a.u. The left and right figures are plotted with the regions of R = 0.0–20.0 a.u. and R = 0.0–100.0 a.u., respectively.

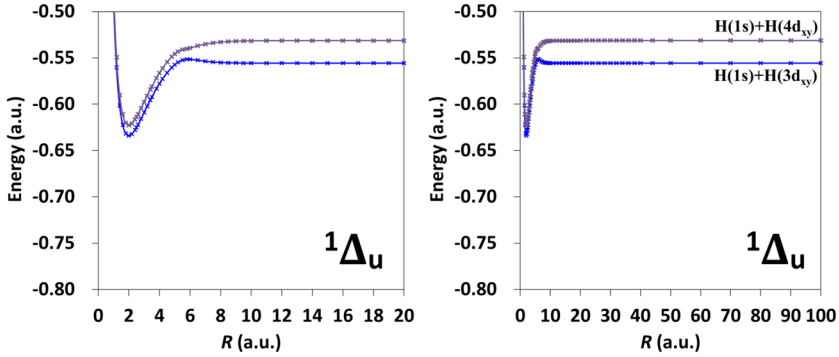

FIG. 11. Potential energy curves of the two lower excited states of $^1\Delta_u$ with the energy region of −0.5 to −0.8 a.u. The left and right figures are plotted with the regions of R = 0.0–20.0 a.u. and R = 0.0–100.0 a.u., respectively.

A. Ground and excited states of the $^1\Sigma_g^+$ symmetry

Since the Σ symmetries, especially $^1\Sigma_g^+$ including the ground state, are the most important both experimentally and theoretically, their ground and excited states have been investigated in many literature.[6,7,15,19–21,36,37] Table I and Table S1 summarize the numerical data of calculated energies for $^1\Sigma_g^+$. For the $1^1\Sigma_g^+$ ground state, the calculated energy by this work was −1.174 474 33 a.u. at the equilibrium distance R = 1.4011 a.u. The energy difference ΔE was 1.601 × 10^{-6} a.u. (0.35 cm^{-1}) from that obtained by Pachucki, whose energy should be variationally the best at this moment.[20] Thus, even using a sampling methodology, absolute energies by the FC-LSE method were sufficiently accurate. In Table I,

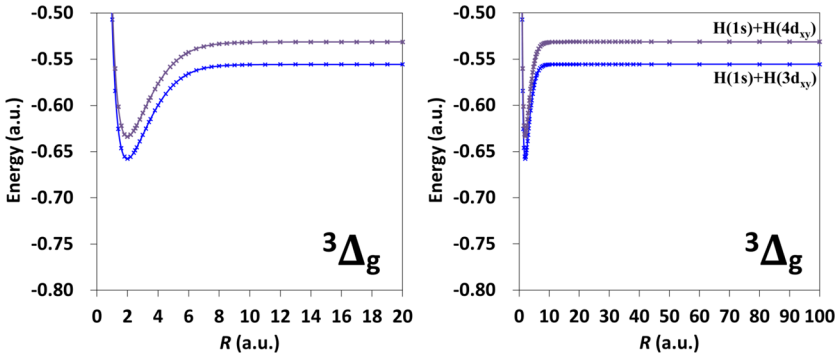

FIG. 12. Potential energy curves of the two lower excited states of $^3\Delta_g$ with the energy region of −0.5 to −0.8 a.u. The left and right figures are plotted with the regions of R = 0.0–20.0 a.u. and R = 0.0–100.0 a.u., respectively.

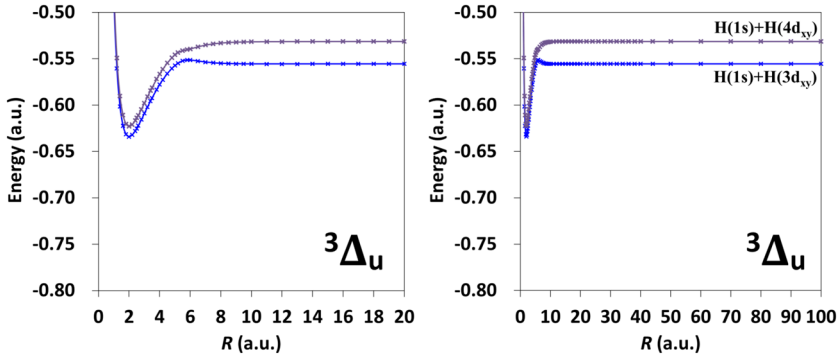

FIG. 13. Potential energy curves of the two lower excited states of $^3\Delta_u$ with the energy region of −0.5 to −0.8 a.u. The left and right figures are plotted with the regions of R = 0.0–20.0 a.u. and R = 0.0–100.0 a.u., respectively.

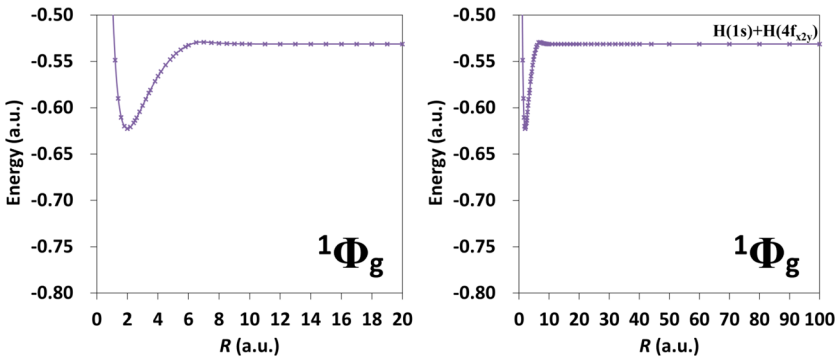

FIG. 14. Potential energy curves of the lowest excited state of $^1\Phi_g$ with the energy region of −0.5 to −0.8 a.u. The left and right figures are plotted with the regions of R = 0.0–20.0 a.u. and R = 0.0–100.0 a.u., respectively.

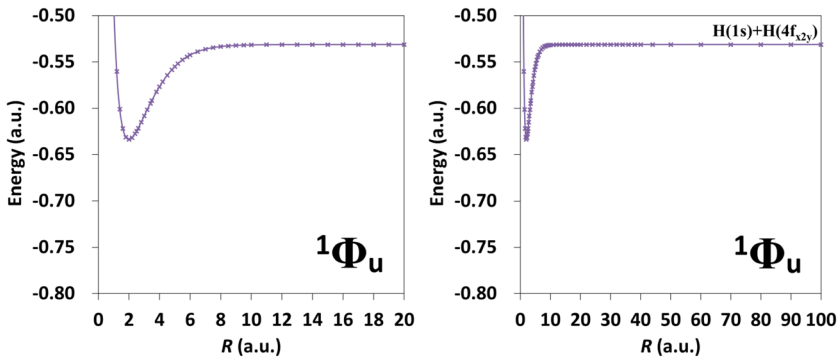

FIG. 15. Potential energy curves of the lowest excited state of $^1\Phi_u$ with the energy region of −0.5 to −0.8 a.u. The left and right figures are plotted with the regions of R = 0.0–20.0 a.u. and R = 0.0–100.0 a.u., respectively.

the results of the excited states $2^1\Sigma_g^+$ to $6^1\Sigma_g^+$ called *EF*, *GK*, *HH*, *P*, and *O*, respectively, are also summarized at several R. These are the conventional spectroscopic notations. The two-character states EF, GK, and HH denote the double minimum potential energy curves. For all these states, ΔE, where Pachucki's results are available,[21] were also equal or less than 10^{-6} hartree order satisfying spectroscopic accuracy almost less than 1 cm^{-1}. Since the dissociation limits are represented as the exact solutions of the hydrogen atoms, the results generally become accurate when approaching to the dissociations. Wolniewicz and Dressler[6,7] reported the very accurate results at many R up to higher excited states. Their solutions were also accurate, but we only suspect a mistype or miscalculation at R = 20.0 a.u. in $4^1\Sigma_g^+$. In comparison with Wolniewicz and Dressler,[6] although some ΔE were 10^{-4} hartree order at some R in $5^1\Sigma_g^+$ and $6^1\Sigma_g^+$, the results in this

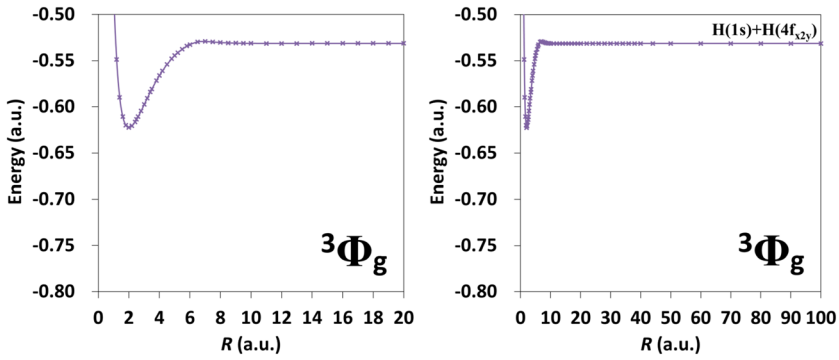

FIG. 16. Potential energy curves of the lowest excited state of $^3\Phi_g$ with the energy region of −0.5 to −0.8 a.u. The left and right figures are plotted with the regions of R = 0.0–20.0 a.u. and R = 0.0–100.0 a.u., respectively.

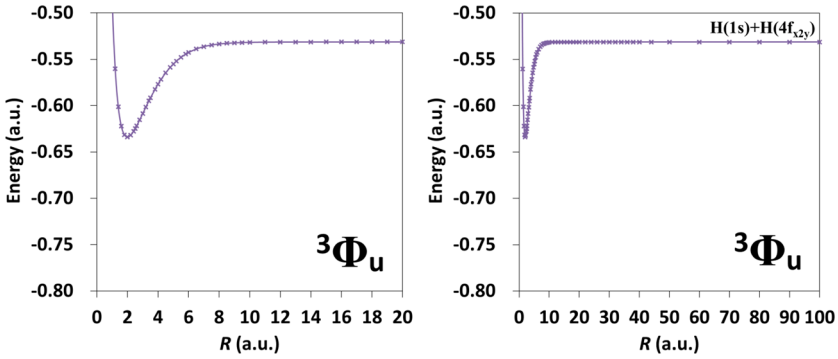

FIG. 17. Potential energy curves of the lowest excited state of $^3\Phi_u$ with the energy region of −0.5 to −0.8 a.u. The left and right figures are plotted with the regions of R = 0.0–20.0 a.u. and R = 0.0–100.0 a.u., respectively.

paper should be better than the ones of Ref. 6, which are much older.

Clementi *et al.* also reported whole range potential energy curves of the 15 $^1\Sigma_g^+$ states and performed the density analysis of them. Although their potential energy curves from the united atom regions to the dissociations are quite reliable, the errors as their absolute energies appeared on 10^{-4} hartree order due to the lack of r_{12} terms. With the LSE method, the H-square errors are available as a good judgment tool for the accurateness of the wave function. As shown in Table S1, the H-square errors of $^1\Sigma_g^+$ states were almost the same order among all the states at similar inter-nuclear distances R. It indicates that all the states are described with the same quality and, therefore, relative quantities such as excitation energy should be also reliable in the FC-LSE method. This is because the overlap and Hamiltonian orthogonalities are ensured in the present calculations.

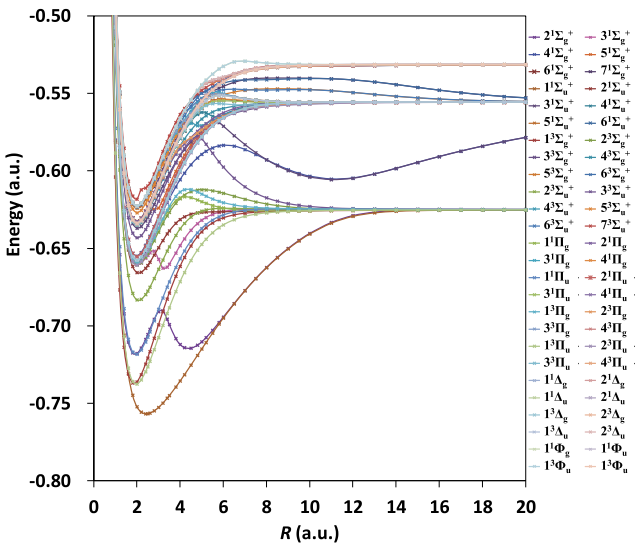

FIG. 18. All 54 states' potential energy curves of $^1\Sigma_g^+$, $^1\Sigma_u^+$, $^3\Sigma_g^+$, $^3\Sigma_u^+$, $^1\Pi_g$, $^1\Pi_u$, $^3\Pi_g$, $^3\Pi_u$, $^1\Delta_g$, $^1\Delta_u$, $^3\Delta_g$, $^3\Delta_u$, $^1\Phi_g$, $^1\Phi_u$, $^3\Phi_g$, and $^3\Phi_u$ symmetries with the energy region of −0.5 to −0.8 a.u. Only the lowest states of $^1\Sigma_g^+$ and $^3\Sigma_u^+$ are excluded since they locate the lower energy region. The figure is plotted with the region of R = 0.0–20.0 a.u.

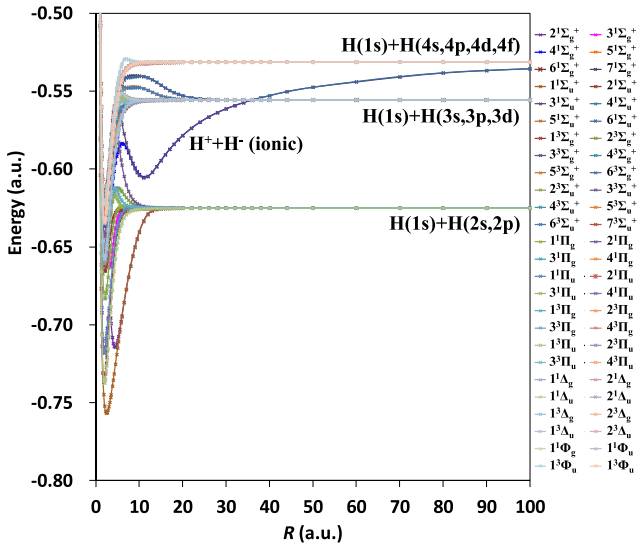

FIG. 19. All 54 states' potential energy curves of $^1\Sigma_g^+$, $^1\Sigma_u^+$, $^3\Sigma_g^+$, $^3\Sigma_u^+$, $^1\Pi_g$, $^1\Pi_u$, $^3\Pi_g$, $^3\Pi_u$, $^1\Delta_g$, $^1\Delta_u$, $^3\Delta_g$, $^3\Delta_u$, $^1\Phi_g$, $^1\Phi_u$, $^3\Phi_g$, and $^3\Phi_u$ symmetries with the energy region of −0.5 to −0.8 a.u. Only the lowest states of $^1\Sigma_g^+$ and $^3\Sigma_u^+$ are excluded since they locate the lower energy region. The figure is plotted with the region of R = 0.0–100.0 a.u.

TABLE I. Comparisons of the absolute energies (a.u.) by this work and the references at several inter-nuclear distances R for the $^1\Sigma_g^+$ symmetry. All the calculated energies on the potential energy curves are given in the supplementary material.

State	R (a.u.)[a]	FC-LSE (this work)	$\Delta E = E_{\text{FC-LSE}} - E_{\text{Ref.}}$[b]	Wolniewicz *et al.*[c]	Sims and Hagstrom *et al.*[d]	Pachucki[e]	Clementi *et al.*[f]
$1^1\Sigma_g^+$ (X)	1.2	−1.164 932 36	2.883×10^{-6}	−1.164 935 241 876	−1.164 935 243 440 028 1	−1.164 935 243 440 309 9(7)	−1.164 66
	1.4011	−1.174 474 33	1.601×10^{-6}	−1.174 475 930 742	−1.174 475 931 399 84	−1.174 475 931 400 216 7(3)	
	1.6	−1.168 584 24	-8.666×10^{-7}	−1.168 583 371 916	−1.168 583 373 370 926 3	−1.168 583 373 371 459 3(8)	
	2.0	−1.138 131 91	1.047×10^{-6}	−1.138 132 955 488	−1.138 132 957 131 503 5	−1.138 132 957 132 648 0(34)	−1.137 89
	3.0	−1.057 327 92	-1.651×10^{-6}	−1.057 326 265 285	−1.057 326 268 869 243 9	−1.057 326 268 872 661 7(70)	−1.057 13
	4.0	−1.016 389 65	6.030×10^{-7}	−1.016 390 251 364	−1.016 390 252 947 128 3	−1.016 390 252 950 668 1(55)	−1.016 26
	6.0	−1.000 835 79	-8.234×10^{-8}	−1.000 835 707 231	−1.000 835 707 654 227 9	−1.000 835 707 655 180 4(23)	−1.168 33
	8.0	−1.000 055 62	-1.503×10^{-8}	−1.000 055 604 837		−1.000 055 604 973 073 0(4)	−1.000 05
	10.0	−1.000 008 77	-1.425×10^{-8}			−1.000 008 755 746 051 5(1)	−1.000 01
	12.0	−1.000 002 54	5.970×10^{-9}			−1.000 002 545 969 528 5(1)	−1.000 00
	16.0	−1.000 000 42	-4.137×10^{-10}			−1.000 000 419 586 312 2	
	20.0	−1.000 000 11	-3.260×10^{-9}			−1.000 000 106 740 128 3	−1.000 00
	30.0	−1.000 000 01					−1.000 00
	50.0	−1.000 000 00					−1.000 00
	100.0	−1.000 000 00					−1.000 00
$2^1\Sigma_g^+$ (EF)	1.2	−0.653 979 28					−0.653 94
	1.6	−0.710 342 22					−0.710 30
	2.0	−0.717 724 70		−0.717 714 276			−0.717 68
	3.0	−0.690 746 80	2.563×10^{-7}	−0.690 746 690		−0.690 747 056 3	−0.690 70
	4.0	−0.711 884 91					−0.711 61
	6.0	−0.694 268 41	-1.381×10^{-6}	−0.694 263 365		−0.694 267 029	
	8.0	−0.662 220 74		−0.662 216 015			−0.661 97
	10.0	−0.640 256 38		−0.640 246 025			−0.640 11
	12.0	−0.628 742 05	-3.800×10^{-8}	−0.628 730 759		−0.628 742 088	−0.628 69
	16.0	−0.625 079 18					
	20.0	−0.625 005 64		−0.625 005 430			−0.625 01
	30.0	−0.625 000 32					−0.625 00
	50.0	−0.625 000 01					−0.625 00
	100.0	−0.625 000 00					−0.625 00
$3^1\Sigma_g^+$ (GK)	1.2	−0.585 297 65					−0.585 24
	1.6	−0.647 812 35					−0.647 78
	2.0	−0.660 443 58		−0.660 428 175			−0.660 42
	3.0	−0.656 985 12	8.250×10^{-7}	−0.656 983 847		−0.656 985 945	−0.656 84
	4.0	−0.648 202 15		−0.648 202 826			−0.648 11
	6.0	−0.626 148 19	-2.210×10^{-7}	−0.626 147 852		−0.626 147 969	
	8.0	−0.624 553 17		−0.624 553 229			−0.624 54
	10.0	−0.624 641 26		−0.624 641 106			−0.624 64
	12.0	−0.624 745 62	3.300×10^{-8}			−0.624 745 653	−0.624 74
	16.0	−0.624 793 69					
	20.0	−0.624 867 18		−0.624 866 924			−0.624 87
	30.0	−0.624 959 19					−0.624 96
	50.0	−0.624 991 13					−0.624 99
	100.0	−0.624 998 89					−0.625 00
$4^1\Sigma_g^+$ (HH)	1.2	−0.584 344 97					−0.584 26
	1.6	−0.644 571 78					−0.644 54
	2.0	−0.654 928 46		−0.654 926 063			−0.654 91
	3.0	−0.630 550 34	3.794×10^{-6}	−0.630 550 821		−0.630 554 134	−0.630 52
	4.0	−0.605 657 88		−0.605 654 911			−0.605 60
	6.0	−0.583 464 51	-9.360×10^{-7}	−0.583 461 341		−0.583 463 574	
	8.0	−0.592 842 06		−0.592 840 002			−0.592 69
	10.0	−0.603 419 20		−0.603 407 271			−0.603 27
	12.0	−0.604 584 76	-4.800×10^{-7}	−0.604 529 322		−0.604 584 280	−0.604 41
	16.0	−0.590 773 08					
	20.0	−0.578 454 87		−0.570 324 253[g]			−0.578 27
	30.0	−0.561 299 77					−0.561 09
	50.0	−0.555 555 67					−0.555 55
	100.0	−0.555 555 56					−0.555 55

TABLE I. (*Continued.*)

State	R (a.u.)[a]	FC-LSE (this work)	$\Delta E = E_{\text{FC-LSE}} - E_{\text{Ref.}}$[b]	Wolniewicz *et al.*[c]	Sims and Hagstrom *et al.*[d]	Pachucki[e]	Clementi *et al.*[f]
$5^1\Sigma_g^+$ (P)	1.2	−0.560 582 84		−0.560 528 775			−0.560 51
	1.6	−0.622 806 31		−0.622 744 249			−0.622 73
	2.0	−0.634 924 12		−0.634 885 512			−0.634 88
	3.0	−0.623 917 63	5.105×10^{-6}	−0.623 917 301		−0.623 922 735	−0.623 87
	4.0	−0.594 768 31		−0.594 768 919			−0.594 73
	6.0	−0.564 424 24	3.340×10^{-7}	−0.564 423 608		−0.564 424 574	
	8.0	−0.557 571 47		−0.557 570 885			−0.557 53
	10.0	−0.556 001 07		−0.556 000 540			−0.555 97
	12.0	−0.555 682 16	9.600×10^{-8}			−0.555 682 256	−0.555 66
	16.0	−0.555 579 88					
	20.0	−0.555 562 77		−0.555 562 684			−0.555 55
	30.0	−0.555 556 24					−0.555 55
	50.0	−0.555 555 59					−0.555 54
	100.0	−0.555 555 56					−0.555 54
$6^1\Sigma_g^+$ (O)	1.2	−0.560 168 89		−0.560 087 944			−0.560 03
	1.6	−0.621 338 43		−0.621 334 070			−0.621 29
	2.0	−0.632 475 06		−0.632 457 557			−0.632 42
	3.0	−0.607 983 35	1.163×10^{-6}	−0.607 841 139		−0.607 984 513	−0.607 93
	4.0	−0.578 872 23		−0.578 810 210			−0.578 80
	6.0	−0.553 905 61	-3.380×10^{-7}	−0.553 862 823		−0.553 905 272	
	8.0	−0.555 462 99		−0.555 460 283			−0.555 42
	10.0	−0.555 539 34		−0.555 538 599			−0.531 32
	12.0	−0.555 533 64	8.100×10^{-8}			−0.555 533 721	−0.555 52
	16.0	−0.555 538 61					
	20.0	−0.555 545 12		−0.555 545 150			−0.555 53
	30.0	−0.555 552 21					−0.555 53
	50.0	−0.555 554 22					−0.555 53
	100.0	−0.555 555 38					−0.555 52

[a]Inter-nuclear distance.
[b]Energy differences between the energies by the FC-LSE method and reference: $\Delta E = E_{\text{FC-LSE}} - E_{\text{Ref.}}$ (a.u.), compared to Refs. 20 and 21 where their reference values are provided.
[c]References 6 and 7.
[d]Reference 15.
[e]Extrapolation energy for $1^1\Sigma_g^+$ (X) in Refs. 20 and 21 for the other states.
[f]Reference 19.
[g]Suspect a mistype or miscalculation in the reference.

We draw the potential energy curve of the ground state $1^1\Sigma_g^+$ in Fig. 1 and this state smoothly dissociates to H(1s) + H(1s). Figure 2 includes all the other excited states $2^1\Sigma_g^+$ to $7^1\Sigma_g^+$, which dissociate to H(1s) + H(2s), H(1s) + H($2p_z$), H(1s) + H(3s), H(1s) + H($3p_z$), H(1s) + H($3d_{z2}$), and H(1s) + H(4s), respectively. Since the ionic curve that dissociates to H^- + H^+ exists in $^1\Sigma_g^+$, the potential energy curves of these excited states become complicated. Since this ionic curve indicates a long-range behavior proportional to $1/R$ which is rather simple, the ionic contribution moves from lower states to higher states, step by step. The potential energy curve of $2^1\Sigma_g^+(EF)$ showed a typical double well potential having the local minimums around R = 2.0 and 4.5 a.u. and the global minimum position was a smaller one, R = 2.0 a.u. As understandable from the right-hand side of Fig. 2, the ionic contribution appeared in the region from R = 4.0 to 10 a.u. On the other hand, although the potential energy curve of $3^1\Sigma_g^+(GK)$ also indicated a double well potential having the local minimums around R = 2.0 and 3.2 a.u., the global minimum position was a larger one, R = 3.2 a.u. This state is not much influenced by the ionic contribution since it dissociates to H(1s) + H($2p_z$) and is symmetrically orthogonal to the ionic S state of H^- in large R. This double well potential, therefore, rather comes from the state repulsion to $2^1\Sigma_g^+(EF)$. The state $4^1\Sigma_g^+(HH)$ has the lowest energy minimum around R = 2.0 a.u. and a local minimum around R = 11.0 a.u. in a broad curve. This state shows a typical ionic nature proportional to $1/R$ from R = 10.0 to R = 37.0 a.u. The complement functions from covalent initial functions only can cover the ionic contribution if one increases the FC order. Introducing an ionic-type initial function, however, is practically important to describe $4^1\Sigma_g^+(HH)$ efficiently at the lower FC order since this state is on the ionic $1/R$ curve around equilibrium. The potential energy curves of $5^1\Sigma_g^+(P)$ and $6^1\Sigma_g^+(O)$ dissociate to H(1s)

+ H($3p_z$) and H(1s) + H($3d_{z2}$), respectively, and they are also symmetrically orthogonal to the ionic state in large R. Therefore, they were almost free from the ionic contribution. There were small shoulders and humps around R = 2.0–6.0 a.u. due to the state repulsions, where many states exist in the small energy region. The state $7^1\Sigma_g^+$ has a nature to dissociate to mixed H(1s) + H(3s) and H(1s) + H(4s) before R = 20.0. a.u. and almost H(1s) + H(3s) before R = 37.0 a.u. However, after the intersystem crossing with $4^1\Sigma_g^+(HH)$ around R = 37.0 a.u., its nature changed from H(1s) + H(3s) to the ionic state. After R = 37.0 a.u., $4^1\Sigma_g^+(HH)$ goes to the dissociation of H(1s) + H(3s). As discussed in Ref. 19, this state finally goes to H(1s) + H(4s) after the intersystem crossing with the higher state. As shown in Table S1, the H-square errors of $4^1\Sigma_g^+(HH)$ became suddenly small after R = 38.0 a.u. By contrast, the H-square errors of $7^1\Sigma_g^+$ became large after R = 36.0 a.u. since the dissociation of H^-H^+ is not exact. Thus, also from the H-square errors, one can recognize that their natures of the ionic state and H(1s) + H(3s) exchange each other.

B. Excited states of the $^1\Sigma_u^+$ symmetry

In the states of $^1\Sigma_u^+$, the ionic contribution $H^- + H^+$ exists but there is no state that dissociates to H(1s) + H(1s) since it is impossible to satisfy both the spatial antisymmetry and singlet spin state at this dissociation. As given in Fig. 3, $1^1\Sigma_u^+(B)$, $2^1\Sigma_u^+(B')$, $3^1\Sigma_u^+(B''B)$, $4^1\Sigma_u^+$, $5^1\Sigma_u^+$, and $6^1\Sigma_u^+$ dissociate to H(1s) + H(2s), H(1s) + H($2p_z$), H(1s) + H(3s), H(1s) + H($3p_z$), H(1s) + H($3d_{z2}$), and H(1s) + H(4s), respectively. As shown in Table S2, these potential energy curves were also in very good agreement with those by Wolniewicz *et al.*[11] Shapes of these potential energy curves look similar to those of $^1\Sigma_g^+$ but there are also noticeable differences. The potential energy curve of $1^1\Sigma_u^+(B)$ has the single minimum around R = 2.4 a.u. although the corresponding $2^1\Sigma_g^+(EF)$ state indicated a double well potential. This potential well was quite broad due to the ionic contribution. The potential energy curve of $2^1\Sigma_u^+(B')$ also indicated a single minimum curve with the minimum around R = 2.0 a.u. although its corresponding $3^1\Sigma_g^+(GK)$ had the double minimums. These would be explained by the nature of weak bonding due to the spatial antisymmety of ungerade symmetry. From the orthogonality between H(1s) + H($2p_z$) and the ionic H^-, $2^1\Sigma_u^+(B')$ is unaffected by the ionic contribution. Similar to the case in $4^1\Sigma_g^+(HH)$, the state $3^1\Sigma_u^+(B''B)$ indicated a typical ionic curve proportional to $1/R$ from R = 10.0 to R = 37.0 a.u. Interestingly, this state has the minimum around R = 2.0 a.u. with the nature of H(1s) + H(3s) before R = 5.5 a.u., where there is a peak with the state repulsion to $4^1\Sigma_u^+$. After R = 5.5 a.u., the energy of this state decreases to acquire the ionic character with the broad minimum around R = 11.0 a.u. Since the potential energy curves of $4^1\Sigma_u^+$ and $5^1\Sigma_u^+$ dissociate to H(1s) + H($3p_z$) and H(1s) + H($3d_{z2}$), respectively, which are orthogonal to H^- at dissociation, they are not influenced by the ionic character. The state $6^1\Sigma_u^+$ also has the nature of mixed H(1s) + H(3s) and H(1s) + H(4s) before R = 20.0. a.u. and almost H(1s) + H(3s) before R = 37.0 a.u. Among the potential energy curves of $3^1\Sigma_u^+$ to $6^1\Sigma_u^+$, there were also small shoulders and humps around R = 2.0–6.0 a.u. due to their state repulsions in the small energy region. Similar to the case in $^1\Sigma_g^+$, the natures of $3^1\Sigma_u^+(B''B)$ and $6^1\Sigma_u^+$ exchange each other around R = 37.0 a.u. This behavior was also observed in the H-square errors given in Table S2, where the H-square errors of $3^1\Sigma_u^+(B''B)$ get better after R = 38.0 a.u., and those of $6^1\Sigma_u^+$ get worse after R = 36.0 a.u. Wolniewicz *et al.* precisely studied these excited states of $^1\Sigma_u^+$ especially for $6^1\Sigma_u^+$ up to very long distance larger than R = 37.0 a.u.[11] Beyond R = 40.0 a.u., the energies of $6^1\Sigma_u^+$ were not especially accurate in our calculations since higher diffuse functions like H(5s) were not included. Nevertheless, their accuracies keep almost within 1 kcal/mol, compared to those from the work of Wolniewicz *et al.*[11]

C. Excited states of the $^3\Sigma_g^+$ and $^3\Sigma_u^+$ symmetries

In the states of $^3\Sigma_g^+$ and $^3\Sigma_u^+$, there is no ionic contribution due to triplet spin where two electrons cannot occupy the same 1s orbital in H^-. Their potential curves, therefore, are simpler than those of $^1\Sigma_g^+$ and $^1\Sigma_u^+$. There is also no state that dissociates to H(1s) + H(1s) in $^3\Sigma_g^+$, but it exists in $^3\Sigma_u^+$. As shown in Fig. 1, the potential energy curve of $1^3\Sigma_u^+$ was mostly repulsive but a very weak energy minimum was observed around R = 8.0 a.u. with its binding energy being 20 μ hartree. This would be due to a dispersion interaction like a van der Waals interaction.

Thus, $1^3\Sigma_g^+$ to $6^1\Sigma_g^+$ and $2^3\Sigma_u^+$ to $7^1\Sigma_u^+$ dissociate to H(1s) + H(2s), H(1s) + H($2p_z$), H(1s) + H(3s), H(1s) + H($3p_z$), H(1s) + H($3d_{z2}$), and H(1s) + H(4s), respectively. Their potential energy curves are given in Figs. 4 and 5 for $^3\Sigma_g^+$ and $^3\Sigma_u^+$, respectively. These are also in very good agreement with those by Wolniewicz and Staszewska[10] as given in Tables S3 and S4. Generally speaking, the binding energies of the states of $^3\Sigma_g^+$ are larger than those of $^3\Sigma_u^+$ since spatially symmetric $^3\Sigma_g^+$ forgives an overlap of the atomic orbitals located in each H. So, the binding energy of $1^3\Sigma_g^+$ to the dissociation was quite larger than that of $2^3\Sigma_u^+$. The potential energy curve of $2^3\Sigma_u^+$ having higher energy upheaves the higher state $3^3\Sigma_u^+$ and this causes a state repulsion around R = 4.8 a.u. between $3^3\Sigma_u^+$ and $4^3\Sigma_u^+$. There was no such a state repulsion between $2^3\Sigma_u^+$ and $3^3\Sigma_u^+$. Around R = 2.0 a.u., the states of $2^3\Sigma_g^+$ and $3^3\Sigma_g^+$ and those of $4^3\Sigma_g^+$ and $5^3\Sigma_g^+$ were almost degenerate since the Rydberg H(3s), H($3p_z$), and H($3d_{z2}$) contribute similarly but they are orthogonal each other. Such quasidegeneracy was not observed in $^3\Sigma_u^+$.

D. Excited states of the $^1\Pi_g$, $^1\Pi_u$, $^3\Pi_g$, and $^3\Pi_u$ symmetries

For the Π, Δ, and Φ symmetries, both the ionic state H^- + H^+ and the state dissociating to H(1s) + H(1s) are not included. Their potential energy curves, therefore, are further simpler than those of the Σ symmetry. Figures 6–9 represent the potential energy curves of the $^1\Pi_g$, $^1\Pi_u$, $^3\Pi_g$, and $^3\Pi_u$ symmetries. Each of them includes four states that dissociate to H(1s) + H($2p_x$), H(1s) + H($3p_x$), H(1s) + H($3d_{xz}$), and H(1s) + H($4p_x$).

The shapes of the potential energy curves $^1\Pi_g$ and $^3\Pi_g$ look similar and also those of $^1\Pi_u$ and $^3\Pi_u$ resemble each other. Thus, there is no significant difference between singlet and triplet states for higher angular momentum symmetries

because even the lowest state of these symmetries is already a Rydberg excitation of the hydrogen atom and it is spatially diffuse. On the other hand, for the Σ symmetry, the potential shapes of the singlet and triplet states were quite different because the ionic state disarranges the potential energy curves of the singlet states only. In Π symmetry, gerade Π_g represents antibonding character like the π^* orbital and ungerade Π_u represents bonding character like the π orbital. Therefore, the binding energies of the states belonging to $^1\Pi_u$ and $^3\Pi_u$ are larger than those of $^1\Pi_g$ and $^3\Pi_g$. As shown in $^3\Sigma_u^+$, the potential energy curves of $1^1\Pi_g$ and $1^3\Pi_g$ locate in higher energy regions and they upheave the higher states $2^1\Pi_g$ and $2^3\Pi_g$ and trigger some state repulsions observed between R = 4.0 and 8.0 a.u. When one compares the potential energy curves of $^3\Sigma_g^+$ and $^1\Pi_u$ or $^3\Pi_u$, their shapes also have some similarities, but the only difference is the existence of the states which dissociate to the s orbitals (2s, 3s, ...) in $^3\Sigma_g^+$. So, the number of states is smaller in the Π symmetry. The same holds for the potential energy curves of $^3\Sigma_u^+$ and $^1\Pi_g$ or $^3\Pi_g$.

As summarized in Tables S5–S8, Wolniewicz *et al.* also studied these states at various R.[8,10,12] ΔE from the energies reported in these references were almost 10^{-5} hartree order or smaller than it but, for some states at some R, the present results should be more accurate than the ones of the references, which are older.

E. Excited states of the $^1\Delta_g$, $^1\Delta_u$, $^3\Delta_g$, $^3\Delta_u$, $^1\Phi_g$, $^1\Phi_u$, $^3\Phi_g$, and $^3\Phi_u$ symmetries

The potential energy curves of the Δ and Φ symmetries are furthermore simpler than those of the Π symmetry because the states dissociating to p orbitals disappear in the Δ and Φ symmetries and the states dissociating to d orbitals also disappear in the Φ symmetry. Figures 10–13 represent the potential energy curves of the $^1\Delta_g$, $^1\Delta_u$, $^3\Delta_g$, and $^3\Delta_u$ symmetries. Each of them includes two states that dissociate to H(1s) + H($3d_{xy}$) and H(1s) + H($4d_{xy}$). Figures 14–17 show the potential energy curves of the $^1\Phi_g$, $^1\Phi_u$, $^3\Phi_g$, and $^3\Phi_u$ symmetries. Each of them includes one state that dissociates to H(1s) + H($4f_{x2y}$).

About their potential curves, similar discussions to the Π symmetry hold and there is no remarkable speciality. For instance, between the singlet and triplet states, the shapes of the potential energy curves $^1\Delta_g$ and $^3\Delta_g$, $^1\Delta_u$ and $^3\Delta_u$, $^1\Phi_g$ and $^3\Phi_g$, and $^1\Phi_u$ and $^3\Phi_u$ quite resemble each other. Thus, the spin state does not make significant differences. In Δ symmetry, Δ_g and Δ_u have bonding and antibonding characters, respectively. In Φ symmetry, Φ_g and Φ_u have antibonding and bonding characters, respectively. Therefore, similar to the cases of Σ and Π, the potential energy curves of the Δ_u and Φ_g symmetries locate higher energy regions in bonding regions than those of the Δ_g and Φ_u symmetries. They cause some state repulsions in the potential energy curves of the Δ_u and Φ_g symmetries.

As summarized in Tables S9–S16, Wolniewicz reported the results of the $^1\Delta_g$ and $^3\Delta_g$ symmetries at various R.[9] ΔE from these energies in Ref. 9 shows a good correspondence, almost about 10^{-5} hartree order or smaller than it, but, for some states at some R, the present results should also be more accurate. There are no more references about the other states and we first reported them in the present study. Thus, the correct solutions even for higher angular momentum symmetries were also simply obtained.

F. Vertical excitation energies

Vertical excitation spectra of H_2 have been studied experimentally for many years by ultraviolet (UV) spectra, vacuum-ultraviolet (VUV) laser action, etc.[39–45] due to their scientific importance in various scientific fields. However, experimental studies often cause some difficulty since even the lowest excited state of H_2 locates over 10 eV, i.e., in the VUV region. In theoretical studies, besides accurate variational calculations as in the present work, scattering dynamical processes after applied laser pulse have been investigated by the R-matrix method, convergent close-coupling method, etc.[46,47] These experimental and theoretical studies, however, reported only a few low-lying excited states.

In the present study, we computed the vertical excitation energies for the 53 excited states at the equilibrium geometry of the $1^1\Sigma_g^+$ ground state R = 1.4011 a.u. and summarized them in Table II, where the presented values do not include vibrational corrections; if one wants to include them, the vertical excitation energies are shifted by −0.2702 eV corresponding to the zero-point vibrational energy 2179.3(1) cm^{-1} of the ground state.[48] The lowest vertical excited state $1^3\Sigma_u^+$ was found at 10.611 eV. This state is on the dissociation channel to H(1s) + H(1s). The adiabatic lowest excited state is $1^1\Sigma_u^+$, but this low energy derives from the ionic contribution and its minimum position is considerably distant from R = 1.4011 a.u. Almost 2.0 eV above, $1^3\Sigma_g^+$, $1^3\Pi_u$, $1^1\Sigma_u^+$, $2^1\Sigma_g^+$, and $1^1\Pi_u$ states exist at 12.537, 12.729, 12.750, 13.125, and 13.216 eV, respectively, in less than 13.5 eV and these states locate within 1.0 eV and their dissociation limits are H(1s) + H(2s,2p). $2^3\Sigma_u^+$ locates at 14.443 eV and it also dissociates to H(1s) + H(2s,2p) despite the large 1 eV interval after $1^1\Pi_u$. In Σ and Π symmetries, there are dissociation channels to 2s and 2p (principal quantum number n = 2), but, in Δ and Φ symmetries, their lowest dissociations are to 3d (n = 3) and 4f (n = 4), respectively, having high energies. The lowest Δ state, therefore, locates in the higher energy region at 14.939 eV as $1^3\Delta_g$ and this state almost degenerates with $1^1\Delta_g$ at 14.940 eV. Similarly, the lowest Φ state exists as $1^3\Phi_u$ at 15.598 eV and it also almost degenerates with $1^1\Phi_u$. Thus, the differences by spin spates are almost negligible especially for higher angular momentum states and the effects of the Pauli repulsion also become negligible. In the higher energy region, the density of states becomes large and accurate theoretical studies would be more desirable to distinguish these electronic states precisely. In Table II, we also summarized comparisons with the other theoretical studies. The references of accurate variational calculations by Wolniewicz *et al.* and Hagstrom *et al.*[6–12,14] are available but these were calculated at R = 1.4 a.u. Although these reference values were separately reported in different papers,[6–12,14] the present study, on the other hand, systematically provided them on the same theoretical level and more

data were presented than references. The vertical excitation energies by the FC-LSE calculations were in good agreement with those of Refs. 6–12 and 14 with the differences less than 0.01 eV and, for some states, the present results may be more accurate than the reference values. They also agreed well with those by the R-matrix and Convergent close-coupling method[46,47] which reported only a few lower excited states.

TABLE II. Absolute energies and vertical excitation energies by the FC-LSE calculations for all the calculated ground and excited states at the equilibrium geometry (R = 1.4011 a.u.) of the $1^1\Sigma_g^+$ ground state. The results are compared with other studies.

	Absolute energy (a.u.)	Vertical excitation energy (eV)			
State	FC-LSE (this work)	FC-LSE (this work)	Ref. (variational calculations at R = 1.4 a.u.)[a,b,c,d,e,f,g,h]	Ref. (R-matrix method)[i]	Ref. (convergent close-coupling method)[j]
$1^1\Sigma_g^+$	−1.174 474 33				
$1^3\Sigma_u^+$	−0.784 535 74	10.611	10.619[b]	10.45(21)	10.67
$1^3\Sigma_g^+$	−0.713 752 72	12.537	12.540[b]	12.41(15)	12.32
$1^3\Pi_u$	−0.706 702 66	12.729	12.732[b]	12.60(21)	12.56
$1^1\Sigma_u^+$	−0.705 919 72	12.750	12.754[c]	13.15(21)	12.66
$2^1\Sigma_g^+$	−0.692 150 03	13.125		13.25(28)	12.92
$1^1\Pi_u$	−0.688 785 01	13.216	13.220[d]	13.11(21)	13.03
$2^3\Sigma_u^+$	−0.643 694 05	14.443	14.447[b]		
$2^3\Sigma_g^+$	−0.630 442 43	14.804	14.807[b]		
$2^3\Pi_u$	−0.628 928 06	14.845	14.850[b]		
$2^1\Sigma_u^+$	−0.628 825 93	14.848	14.851[c]		
$3^3\Sigma_g^+$	−0.626 655 80	14.907	14.909[b]		
$3^1\Sigma_g^+$	−0.626 602 67	14.908			
$1^3\Pi_g$	−0.626 383 27	14.914	14.918[b]		
$1^1\Pi_g$	−0.626 325 78	14.916	14.920[e]		
$1^3\Delta_g$	−0.625 486 07	14.939	14.944[f]		
$1^1\Delta_g$	−0.625 426 45	14.940	14.945[f]		
$4^1\Sigma_g^+$	−0.624 540 82	14.964			
$2^1\Pi_u$	−0.623 754 41	14.986	14.990[d]		
$3^3\Sigma_u^+$	−0.608 265 32	15.407	15.412[b]		
$4^3\Sigma_g^+$	−0.603 304 84	15.542	15.547[g]		
$3^1\Sigma_u^+$	−0.602 737 56	15.558	15.562[c]		
$3^3\Pi_u$	−0.602 700 33	15.559	15.563[b]		
$5^3\Sigma_g^+$	−0.601 830 74	15.582	15.586[g]		
$5^1\Sigma_g^+$	−0.601 797 60	15.583	15.588[h]		
$2^3\Pi_g$	−0.601 679 23	15.587	15.590[b]		
$2^1\Pi_g$	−0.601 649 04	15.587	15.591[e]		
$1^1\Delta_u$	−0.601 476 63	15.592			
$1^3\Delta_u$	−0.601 473 87	15.592			
$4^3\Pi_u$	−0.601 451 09	15.593			
$3^1\Pi_u$	−0.601 450 28	15.593	15.596[d]		
$4^1\Sigma_u^+$	−0.601 422 19	15.594	15.596[c]		
$4^3\Sigma_u^+$	−0.601 420 94	15.594			
$2^3\Delta_g$	−0.601 334 31	15.596	15.601[f]		
$2^1\Delta_g$	−0.601 295 89	15.597	15.602[f]		
$1^3\Phi_u$	−0.601 275 53	15.598			
$1^1\Phi_u$	−0.601 275 20	15.598			
$6^1\Sigma_g^+$	−0.600 886 53	15.608	15.613[h]		
$4^1\Pi_u$	−0.600 536 63	15.618	15.621[d]		
$5^3\Sigma_u^+$	−0.593 530 90	15.808			
$6^3\Sigma_g^+$	−0.591 350 21	15.868			
$5^1\Sigma_u^+$	−0.590 882 45	15.880	15.886[c]		
$7^1\Sigma_g^+$	−0.590 534 25	15.890			
$3^3\Pi_g$	−0.590 208 33	15.899			
$3^1\Pi_g$	−0.590 178 60	15.899			
$2^3\Delta_u$	−0.590 166 29	15.900			
$2^1\Delta_u$	−0.590 160 62	15.900			
$6^3\Sigma_u^+$	−0.590 130 41	15.901			
$6^1\Sigma_u^+$	−0.590 129 29	15.901	15.903[c]		

TABLE II. (*Continued.*)

State	Absolute energy (a.u.)	Vertical excitation energy (eV)			
	FC-LSE (this work)	FC-LSE (this work)	Ref. (variational calculations at $R = 1.4$ a.u.)[a,b,c,d,e,f,g,h]	Ref. (R-matrix method)[i]	Ref. (convergent close-coupling method)[j]
$4^1\Pi_g$	−0.589 996 95	15.904			
$4^3\Pi_g$	−0.589 984 65	15.905			
$1^3\Phi_g$	−0.589 859 17	15.908			
$1^1\Phi_g$	−0.589 851 12	15.908			
$7^3\Sigma_u^+$	−0.585 290 25	16.033			

[a]Reference 7 for the ground-state energy.
[b]Reference 10.
[c]Reference 11.
[d]Reference 12.
[e]Reference 8.
[f]Reference 9.
[g]Reference 14.
[h]Reference 6.
[i]Reference 46.
[j]Reference 47.

IV. CONCLUSIONS

The accurate potential energy curves of the ground and excited states (total 54 states) for the $^1\Sigma_g^+$, $^1\Sigma_u^+$, $^3\Sigma_g^+$, $^3\Sigma_u^+$, $^1\Pi_g$, $^1\Pi_u$, $^3\Pi_g$, $^3\Pi_u$, $^1\Delta_g$, $^1\Delta_u$, $^3\Delta_g$, $^3\Delta_u$, $^1\Phi_g$, $^1\Phi_u$, $^3\Phi_g$, and $^3\Phi_u$ symmetries were theoretically obtained by the FC theory with the sampling-type integral-free LSE method instead of the variational method. We prepared the initial functions represented as the HLSP type from hydrogen-atom wave functions, which guarantee the correct dissociations to atoms for all the target states. The calculated potential energy curves were accurate and smooth as not only relative shapes but also absolute energies almost satisfying spectroscopic accuracy. Compared to the variational methods that require analytical integrations, the LSE calculations were performed with lower computational cost and were highly efficiently parallelized. For practical calculations in the LSE method, however, it is significant to generate appropriate sampling points for the target states as much as possible.

In the present study, we performed a comprehensive study to understand the potential energy curves of H_2 with accurate solutions of the SE, from equilibrium to dissociation, and from the ground and low-lying excited states up to higher angular momentum symmetries. There is no such inclusive study in the literature even for the simple H_2 molecule. By looking at all the potential curves and comparing them concurrently, we could systematically understand the physical natures of their states and potential energy curves. For example, the potential energy curves in the $^1\Sigma_g^+$ and $^1\Sigma_u^+$ symmetries showed some complicated behaviors due to the existence of the ionic state. On the other hand, there is no such complexity for the other symmetries. The present study first reported some potential energy curves of the higher excited states belonging to higher angular momentum symmetries. We also examined the vertical excitation energies at the equilibrium geometry of the $1^1\Sigma_g^+$ ground state. Thus, the data presented in this study may be valuable as a theoretical database. The present study is one of the simple and clear examples in which the FC theory and the LSE method are used as a reliable tool to study not only ground but also excited states and their potential energy curves.

SUPPLEMENTARY MATERIAL

See supplementary material for the numerical data of the potential energy curves and their plots for all the calculated states.

ACKNOWLEDGMENTS

The authors thank Mr. Nobuo Kawakami for his support to the research in QCRI, and the computer centers of the Research Center for Computational Science, Okazaki, Japan, for their generous support and encouragement. This research also used computational resources of the K computer provided by the RIKEN Advanced Institute for Computational Science, Kobe, Japan, through the HPCI System Research project (Project No. hp140140) and TSUBAME at the Tokyo Institute of Technology, Tokyo, Japan. This work was also supported by JSPS KAKENHI (Grant Nos. 26108516, 16H00943, 16H02257, 17H04867, and 17H06233).

[1]W. Heitler and F. London, Z. Phys. **44**, 455 (1927).
[2]H. M. James and A. S. Coolidge, J. Chem. Phys. **1**, 825 (1933); **3**, 129 (1935).
[3]W. Kolos and C. C. Roothaan, Rev. Mod. Phys. **32**, 205 (1960); **32**, 219 (1960).
[4]E. R. Davidson, J. Chem. Phys. **35**, 1189 (1961).
[5]W. Kolos and L. Wolniewicz, J. Chem. Phys. **41**, 3663 (1964); **43**, 2429 (1965); Chem. Phys. Lett. **24**, 457 (1974); W. Kolos, J. Chem. Phys. **101**, 1330 (1994); L. Wolniewicz, *ibid.* **99**, 1851 (1993).
[6]L. Wolniewicz and K. Dressler, J. Chem. Phys. **100**, 444 (1994).
[7]L. Wolniewicz, J. Chem. Phys. **103**, 1792 (1995).
[8]L. Wolniewicz, J. Mol. Spectrosc. **169**, 329 (1995).
[9]L. Wolniewicz, J. Mol. Spectrosc. **174**, 132 (1995).
[10]G. Staszewska and L. Wolniewicz, J. Mol. Spectrosc. **198**, 416 (1999).
[11]G. Staszewska and L. Wolniewicz, J. Mol. Spectrosc. **212**, 208 (2002).
[12]L. Wolniewicz and G. Staszewska, J. Mol. Spectrosc. **220**, 45 (2003).
[13]J. W. Liu and S. Hagstrom, Phys. Rev. A **48**, 166 (1993).
[14]J. W. Liu and S. Hagstrom, J. Phys. B: At., Mol. Opt. Phys. **27**, L729 (1994).
[15]J. S. Sims and S. Hagstrom, J. Chem. Phys. **124**, 094101 (2006).

[16]J. Rychlewski, W. Cencek, and J. Komasa, Chem. Phys. Lett. **229**, 657 (1994).
[17]W. Cencek and W. Kutzelnigg, J. Chem. Phys. **105**, 5878 (1996).
[18]W. Cencek and K. Szalewicz, Int. J. Quantum Chem. **108**, 2191 (2008).
[19]G. Corongiu and E. Clementi, J. Chem. Phys. **131**, 034301 (2009).
[20]K. Pachucki, Phys. Rev. A **82**, 032509 (2010).
[21]K. Pachucki, Phys. Rev. A **88**, 022507 (2013).
[22]E. A. Hylleraas, Z. Phys. **54**, 347 (1929).
[23]H. Nakatsuji, J. Chem. Phys. **113**, 2949 (2000).
[24]H. Nakatsuji, Phys. Rev. Lett. **93**, 030403 (2004).
[25]H. Nakatsuji, Phys. Rev. A **72**, 062110 (2005).
[26]H. Nakatsuji, H. Nakashima, Y. Kurokawa, and A. Ishikawa, Phys. Rev. Lett. **99**, 240402 (2007).
[27]H. Nakatsuji, Acc. Chem. Res. **45**, 1480 (2012).
[28]H. Nakashima and H. Nakatsuji, J. Chem. Phys. **139**, 044112 (2013).
[29]H. Nakatsuji and H. Nakashima, J. Chem. Phys. **142**, 084117 (2015).
[30]H. Nakatsuji and H. Nakashima, J. Chem. Phys. **142**, 194101 (2015).
[31]H. Nakashima and H. Nakatsuji, J. Chem. Phys. **127**, 224104 (2007).
[32]A. Bande, H. Nakashima, and H. Nakatsuji, Chem. Phys. Lett. **496**, 347 (2010).
[33]H. Nakatsuji and H. Nakashima, TSUBAME e-Sci. J. **11**(08), 24 (2014).
[34]RCCS Report in Institute for Molecular Science (IMS), No. 17, April 2016-March 2017 (in Japanese).
[35]H. Nakatsuji, H. Nakashima, Y. I. Kurokawa, and T. Miyahara, HPCI Res. Rep. **2**, 39 (2017).
[36]Y. Kurokawa, H. Nakashima, and H. Nakatsuji, Phys. Rev. A **72**, 062502 (2005).
[37]Y. I. Kurokawa, H. Nakashima, and H. Nakatsuji, "Solving the Schrödinger equation of hydrogen molecules with the free-complement variational theory: Essentially exact potential curves and vibrational levels of the ground and excited states of the Σ symmetry," Phys. Chem. Chem. Phys. (published online).
[38]N. Metropolis, A. W. Rosenbluth, M. N. Rosenbluth, A. M. Teller, and E. Teller, J. Chem. Phys. **21**, 1087 (1953).
[39]G. H. Dieke and J. J. Hopfield, Phys. Rev. **30**, 400 (1927).
[40]J. J. Hopfield, Nature **125**, 927 (1930).
[41]A. W. Ali and A. C. Kolb, Appl. Phys. Lett. **13**, 259 (1968).
[42]R. T. Hodgson, Phys. Rev. Lett. **25**, 494 (1970).
[43]T. E. Sharp, At. Data Nucl. Data Tables **2**, 119 (1971).
[44]M. Rothschild, H. Egger, R. T. Hawkins, J. Bokor, H. Pummer, and C. K. Rhodes, Phys. Rev. A **23**, 206 (1981).
[45]A. Palacios, H. Bachau, and F. Martin, Phys. Rev. A **75**, 013408 (2007).
[46]S. E. Branchett, J. Tennyson, and L. A. Morgan, J. Phys. B: At., Mol. Opt. Phys. **23**, 4625 (1990).
[47]M. C. Zammit, J. S. Savage, D. V. Fursa, and I. Bray, Phys. Rev. Lett. **116**, 233201 (2016).
[48]K. K. Irlkura, J. Phys. Chem. Ref. Data **36**, 389 (2007).